Turkish Journal of Physics

Volume 46
Number 6 *SI-6*

Article 2

1-1-2022

Extinction and growth on an inhomogeneous Seascape

TUNG TRAN

MEHRAN KARDAR

TÜBİTAK

Turkish Journal of Physics

http://journals.tubitak.gov.tr/physics/

Research Article

Turk J Phys
(2022) 46: 173 – 187

doi:10.55730/1300-0101.2724

Extinction and growth on an inhomogeneous seascape

Tung X. TRAN, Mehran KARDAR*
Department of Physics, Massachusetts Institute of Technology, Cambridge, U.S.A.

Received: 15.11.2022 • **Accepted/Published Online:** 30.11.2022 • **Final Version:** 27.12.2022

Abstract: The effects of noise and nonuniformity on dynamics of populations are relevant and timely subjects of investigation. One form of variation is the time dependence of the reproduction rate (fitness), referred to as "seascape" noise; another is time-independent intrinsic dependencies of fitness on location (in the parlance of statistical physics, corresponding to annealed and quenched disorder, respectively). The former was studied recently and demonstrated to lead to novel universality classes for extinction and growth. To reduce the gap between this theoretical model and reality, we develop a new formalism for seascape noise where growth and migration parameters are inhomogeneous. In this formalism, we consider several subpopulation classes: each class consists of patches with similar properties, but patches for different classes are different. Employing a generalized mean-field approach, we self-consistently find distributions for numbers of each subpopulation in steady-state. Interestingly, we find that extinction is characterized by a critical exponent which depends on the characteristics of the subpopulation with the largest noise-to-migration ratio, regardless of the relative size of this subpopulation. Growth is now governed by a generalized Richards law, with an effective exponent varying with population size.

Keywords: Population dynamics, growth, extinction, stochasticity, spatial dependence, seascape

1. Introduction

Population dynamics has garnered diverse interest over the past few decades, with appearances in fields such as cancer research [1], forestry [2], pandemic modeling [3], wealth modeling [4], and many others. The multitude of data sets have been fitted to a number of empirical models [5] which call for good justification. Indeed, despite a rich literature on mathematical models for population growth [6–12], this field remains a fertile ground for theoretical explanations of the origins of various empirical models [2]. The simplest model of population growth is the logistic equation:

$$\frac{\mathrm{d}y}{\mathrm{d}t} = \mu y - a y^2 \ , \tag{1.1}$$

describing a population of size $y(t)$ that initially grows exponentially at rate μ (fitness), until resource limitation leads to saturation at $y(t \to \infty) = \mu/a$.

While most empirical models focus on the behavior of an average population, there is underlying stochasticity that must be accounted for. One source of variation is due to the intrinsic randomness

*Correspondence: kardar@mit.edu

in reproduction events (whether a member of the population has zero, one, or several off-springs); this gives rise to the so-called *demographic noise* [13–15] and leads to interesting phenomena such as noise-stabilization [16], reversing the effect of deterministic selection [17], robust pattern formation [18], and rare extinction events [19, 20]. Mathematically, the magnitude of demographic noise is proportional to the square root of the population size, and it is thus most influential in small populations. A typical population is also distributed among a number of different locations, with subpopulation at location i indicated by $y_i(t)$ (for example, birds in archipelagos, microorganisms in soils, and cells in vivo). Including migrations between the different locales, as well as demographic noise, now generalizes Eq. (1.1) to

$$\frac{\mathrm{d}y_i}{\mathrm{d}t} = \mu y_i - a y_i^2 + \sum_j M_{ij}(y_j - y_i) + \sqrt{y_i}\ \eta_i(t)\ , \tag{1.2}$$

with M_{ij} being the rate of migration from patch j and patch i, and $\eta_i(t)$ being a Gaussian noise of zero mean and unit magnitude. (As $\mu \to 0$, the extinction process of the population is known to be described by a corresponding directed percolation universality class [21].)

The focus of this work, however, is on extrinsic (e.g., environmental) factors that cause the reproduction rate itself to vary from location to location, and from time to time. Extending analogy from a random landscape, this type of time-dependent variation is referred to as *seascape noise*. Due to variations of the fitness term, this type of noise is mathematically expressed as a term proportional to the local population size y_i [22, 23], leading to coupled stochastic differential equations of the form

$$\frac{\mathrm{d}y_i}{\mathrm{d}t} = \mu y_i - a y_i^2 + \sum_j M_{ij}(y_j - y_i) + \sigma y_i \eta_i(t)\ , \tag{1.3}$$

with σ^2 being the variance of the seascape noise.

The presence of seascape noise can significantly alter the behavior of the population: Reference [22] considered a "mean-field" setting with complete connections between N sites described by $M_{ij} = D/N$, in the limit of $N \to \infty$. In the absence of seascape noise, it is easy to check that the steady-state mean behaves in the same way as the logistic equation, i.e. $\overline{y} = \sum_{i=1}^{N} y_i/N = \mu/a$. The average population vanishes linearly on approach to the extinction threshold for $\mu \to 0$. If there is no demographic noise, large seascape noise changes the extinction critical behavior from $\overline{y} \propto \mu^1$ to $\overline{y} \propto \mu^\beta$, with a critical exponent $\beta = 2D/\sigma^2$ (for $\sigma^2 > 2D$). Furthermore, in this regime, the probability distribution of the population broadens to the extent that the variance diverges, a feature not present with demographic noise.

There is in principle no reason for the saturation term to take the quadratic form $S(y) = -ay^2$. Indeed, other forms have appeared in the literature, all capturing the same qualitative behavior in which the population size increases monotonically with time and saturates at the root of $\mu y + S(y) = 0$. Notably, the Richards growth equation has $S(y) \propto -y^\gamma$, with a fractional exponent γ fitted to the data [11, 12]. Originally introduced in describing plant growth [24–26], the Richards equation

$$\frac{\mathrm{d}\overline{y}}{\mathrm{d}t} = \mu\overline{y} - a\overline{y}^{\,\gamma}\ , \tag{1.4}$$

has been used in diverse contexts including modeling of pandemics [3, 27–30], bacterial growth [31], marketing [32], fisheries [33–35], forest growth [36–39], and agriculture [40, 41]. However, in the

context of critical phenomena, introducing a nonanalytic term at the outset is not legitimate. It is appropriate to extend the growth law by the inclusion of additional analytic terms in the expansion $S(y) = -ay^2 + a_3y^3 + a_4y^4 + \cdots$, but a nonanalytic term $\propto y^\gamma$ requires justification. In Reference [23], it was shown that Eq. (1.4) emerges naturally upon averaging over migrating populations subject to seascape noise, as in Eq. (1.3) for any such analytic $S(y)$.

While an intriguing connection, the above result [22, 23] relies on the assumption of equivalency between all sites with the same average growth parameters μ and $S(y)$, as well as $M_{ij} = D/N$ for migration between any pair. Even though this is a typical assumption [42–46]), persistent differences between different locales are an important feature of a biological landscape, and can give rise, even in equilibrium, to qualitative long-term, behavioral changes [4, 13, 47–50]. The present work aims to include some effects of persistent inhomogeneity through a generalization of the equivalent neighbor model to include several classes of patches. Patches belonging to each class have identical properties but are distinct from other patches, and migration rates may also depend on pairs of classes. As expected, the behavior of the overall population is influenced by the distinct properties of its subpopulations. Interestingly, the relative size of a subpopulation is less important than the degree of its fitness variability and migration to other subgroups.

The following sections present the above formalism and some of its applications. In Section 2, we analytically derive the steady-state distribution for each class; these are wide, power-law distributions with diverging moments. We construct a set of master consistency equations and use them to find the equilibrium mean population as well as higher moments. In Section 3, we consider an extinction scenario where the average reproduction rate goes to zero and derive the dependence of the population mean on the statistics of the growth and noise factors. To highlight such dependence, we use numerical analysis on the extinction of a population with an "exotic" subpopulation (with a large noise-to-connection ratio). In Section 4, we employ a seasonal-growth model (alternating between growth and migration stages) to explain how Richards-like nonanalyticity emerges from a mean-field theory. Section 5 concludes with an overview.

2. Model & formalism

Our model considers ℓ population classes labeled by a Greek index $\alpha \in \{1, \ldots, \ell\}$. The number of patches in each class is set such that

$$p_\alpha = \lim_{\mathcal{N}\to\infty} \frac{N_\alpha}{\mathcal{N}} \ , \tag{2.1}$$

with N_α being the number of patches in class α, and $\mathcal{N} = \sum_\alpha N_\alpha$ being the total number of patches in the entire population. All patches among a class α have equal average growth parameters μ_α and a_α and are internally fully and equally connected. Next, let $M_{\alpha\beta}$ denote the migration rate between any patch i in class α and any patch j in class β, which is the same for all pairs $i \in \alpha$ and $j \in \beta$. This matrix is symmetric, $M_{\alpha\beta} = M_{\beta\alpha}$, so that the total population is conserved under the effect of migration. We also scale the connection strengths as $M_{\alpha\beta} = D_{\alpha\beta}/\mathcal{N}$ for some fixed $D_{\alpha\beta}$, to obtain a proper limit when $\mathcal{N} \to \infty$.

We then solve for the stationary probability distribution of the subpopulations and their mo-

ments, starting from rewriting Eq. (1.3) for any patch $i \in \alpha$ as

$$\frac{\mathrm{d}y_\alpha^i}{\mathrm{d}t} = \mu_\alpha y_\alpha^i - a_\alpha (y_\alpha^i)^2 + \sum_\beta \sum_{j\in\beta} M_{\alpha\beta}(y_\beta^j - y_\alpha^i) + \sigma_\alpha y_\alpha^i \ \eta_\alpha^i(t) \ . \tag{2.2}$$

In the $\mathcal{N} \to \infty$ limit, $\sum_{j\in\beta} y_\beta^j/\mathcal{N}$ over patches in class β approaches $\overline{y}_\beta \ N_\beta/\mathcal{N}$, such that the above equation becomes

$$\frac{\mathrm{d}y_\alpha^i}{\mathrm{d}t} = \mu_\alpha y_\alpha^i - a_\alpha (y_\alpha^i)^2 + \sum_\beta D_{\alpha\beta} p_\beta (\overline{y}_\beta - y_\alpha^i) + \sigma_\alpha y_\alpha^i \ \eta_\alpha^i(t) \ , \tag{2.3}$$

From the above stochastic equations, we can construct corresponding Fokker-Planck equations for probability distributions $\rho_\alpha(y_\alpha)$, with $\alpha = (1, \cdots, \ell)$, as

$$\frac{\partial \rho_\alpha}{\partial t} = -\partial_{y_\alpha}\left[\Big(\mu_\alpha y_\alpha - a_\alpha y_\alpha^2 + \sum_\beta D_{\alpha\beta} p_\beta (\overline{y}_\beta - y_\alpha)\Big)\rho_\alpha - \frac{\sigma_\alpha^2}{2}\partial_{y_\alpha}(y_\alpha^2 \rho_\alpha)\right] \ . \tag{2.4}$$

The distributions are coupled to each other, but only through the averages $\{\overline{y}_\alpha(t)\}$. The stationary distributions are found by setting the probability currents – the terms in the square parentheses – to 0, which (following division by $\sigma_\alpha^2/2$) leads to the ordinary differential equations

$$0 = y_\alpha^2 \rho_\alpha' + \Big(2 + \sum_\beta C_{D_{\alpha\beta}} p_\beta - C_{\mu_\alpha}\Big) y_\alpha \rho_\alpha - \sum_\beta C_{D_{\alpha\beta}} p_\beta \overline{y}_\beta \rho_\alpha + C_{a_\alpha} y_\alpha^2 \rho_\alpha \ , \tag{2.5}$$

where we have set $C_{D_{\alpha\beta}} = D_{\alpha\beta}/\sigma_\alpha^2$, $C_{\mu_\alpha} = \mu_\alpha/\sigma_\alpha^2$, and $C_{a_\alpha} = 2a_\alpha/\sigma_\alpha^2$. Let us now set

$$\begin{aligned} C_{D_\alpha} &= \sum_\beta C_{D_{\alpha\beta}} p_\beta = \frac{2}{\sigma_\alpha^2} \sum_\beta p_\beta D_{\alpha\beta} \ , \\ (y_0)_\alpha &= \frac{\sum_\beta C_{D_{\alpha\beta}} p_\beta \, \overline{y}_\beta}{\sum_\beta C_{D_{\alpha\beta}} p_\beta} = \frac{\sum_\beta p_\beta D_{\alpha\beta} \, \overline{y}_\beta}{\sum_\beta p_\beta D_{\alpha\beta}} \ , \end{aligned} \tag{2.6}$$

the first is a measure of migrations (into or out of class α to noise in this class; the second is a weighted average of the input to α by migration. In terms of these parameters, the Fokker-Planck equations become

$$0 = y_\alpha^2 \rho_\alpha' + (2 + C_{D_\alpha} - C_{\mu_\alpha}) \, y_\alpha \rho_\alpha - C_{D_\alpha} (y_0)_\alpha \rho_\alpha + C_{a_\alpha} y_\alpha^2 \rho_\alpha \ . \tag{2.7}$$

These equations admit solutions in the form of power-laws with cutoffs at small and large values: a (not normalized) distribution proportional to

$$\hat{\rho}_\alpha(y_\alpha) = e^{-C_{D_\alpha}(y_0)_\alpha / y_\alpha} y_\alpha^{-2 - C_{D_\alpha} + C_{\mu_\alpha}} e^{-C_{a_\alpha} y_\alpha} \ . \tag{2.8}$$

For subgroup α, the upper cutoff, set by C_{a_α} only depends on characteristics of α; the intermediate power-law is influenced by migration to other subgroups through C_{D_α}, while the coupling to average

behaviors of other classes is only felt through the lower cutoff. Integrating over $\hat{\rho}_\alpha(y_\alpha)$ yields the m-th (not normalized) moment

$$\langle y_\alpha^m \rangle = 2 \left[\frac{C_{a_\alpha}}{C_{D_\alpha}(y_0)_\alpha} \right]^{\frac{1+\omega_\alpha - m}{2}} \mathcal{K}_{1+\omega_\alpha - m}(2x_\alpha) \ , \tag{2.9}$$

with $x_\alpha = \sqrt{C_{a_\alpha} C_{D_\alpha}(y_0)_\alpha}$, $\omega_\alpha = C_{D_\alpha} - C_{\mu_\alpha}$, and $\mathcal{K}_\gamma$ being a modified Bessel function of the second kind.

In the $N_\alpha \to \infty$ limit, the empirical mean $\overline{y}_\alpha$ equals the mean of the distribution $\rho_\alpha(y_\alpha)$, given by

$$\overline{y}_\alpha \simeq \langle y_\alpha \rangle = \frac{x_\alpha}{C_{a_\alpha}} \frac{\mathcal{K}_{\omega_\alpha}(2x_\alpha)}{\mathcal{K}_{\omega_\alpha+1}(2x_\alpha)} \ . \tag{2.10}$$

This set of ℓ equations is sufficient to solve, either numerically or analytically under some approximations, for the ℓ unknowns $\overline{y}_\alpha$, which permits the calculations of all higher moments.

In a quasi-steady state, averaging Eq. (2.3) over all patches cancels all noise terms (in the large $\mathcal{N}$ limit) and migration terms (due to their symmetry), resulting in

$$\frac{\mathrm{d}}{\mathrm{d}t} \sum_\alpha p_\alpha \overline{y}_\alpha = \sum_\alpha p_\alpha \mu_\alpha \overline{y}_\alpha - \sum_\alpha p_\alpha a_\alpha \langle y_\alpha^2 \rangle \ , \tag{2.11}$$

suggesting that nonanalytic behaviors emerge from nonanalytic dependence of $\langle y_\alpha^2 \rangle$ on $\overline{y}_\alpha$.

3. Extinction behavior

For a single class, the steady state population $\overline{y}$ vanishes when the net reproduction rate $\mu \to 0$, as $\overline{y} \propto \mu^\beta$. The critical exponent $\beta = 2D/\sigma^2$ is governed by $C_\mu \ll C_D$. For multiple classes with distinct $\{\mu_\alpha\}$ (some of which can be negative), all classes go extinct at the same point, because species with positive growth can act as sources – via migration – to species with negative growth. For simplicity of calculation, we still assume that the range of $\{\mu_\alpha\}$ is much smaller than the scale set by migration. In this limit (as shown below), extinction occurs when the mean growth rate $\overline{\mu} = \sum_\alpha p_\alpha \mu_\alpha$ goes to 0. We further assume that the system has reached the steady state given by Eq. (2.8). The extinction transition is then characterized by the vanishing of $\{\overline{y}_\alpha\}$ as a function of the environmental factors $\{p_\alpha, \mu_\alpha, \sigma_\alpha\}$.

We derive the extinction critical behavior by considering the asymptotic behavior of the right hand side of Eq. (2.10) in the $(y_0)_\alpha \to 0$ limit (or equivalently $x_\alpha \to 0$). Given the nonanalytic power law distribution in Eq. (2.8), it is not surprising that the expansion near $x = 0$ of $\mathcal{K}_\omega / \mathcal{K}_{\omega+1}$ is nonanalytic:

$$\frac{\mathcal{K}_\omega(2x)}{\mathcal{K}_{\omega+1}(2x)} \simeq x \left(\frac{1}{\omega} + \frac{x^2}{\omega^2(1-\omega)} + \frac{\Gamma(-\omega)}{\Gamma(1+\omega)} x^{2\omega} \right) \ . \tag{3.1}$$

In the $x \to 0$ limit, the dominant correction term in the parentheses switches from x^2 for $\omega > 1$ to

$x^{2\omega}$ for $\omega < 1$. Combining this with an approximation for $C_\mu \ll C_D$, we rewrite Eq. (3.2) as

$$\begin{aligned} \overline{y}_\alpha &= (y_0)_\alpha \left[1 + \frac{C_{\mu_\alpha}}{C_{D_\alpha}} - \gamma_\alpha (y_0)_\alpha^{q_\alpha}\right] , \\ q_\alpha &= \min(1, \omega_\alpha) , \\ \gamma_\alpha &= \begin{cases} \frac{C_{a_\alpha} C_{D_\alpha}}{\omega_\alpha(\omega_\alpha - 1)} & \text{if } \omega_\alpha > 1 , \\ -\omega_\alpha \frac{\Gamma(-\omega_\alpha)}{\Gamma(1+\omega_\alpha)} \left(C_{a_\alpha} C_{D_\alpha}\right)^{\omega_\alpha} & \text{if } \omega_\alpha < 1 . \end{cases} \end{aligned} \tag{3.2}$$

As the second and third terms in the square bracket are small corrections, Eq. (3.2) suggests $\overline{y}_\alpha \approx (y_0)_\alpha$ for all α, and therefore

$$\overline{y}_\alpha \approx \overline{y} \text{ for all } \alpha , \tag{3.3}$$

for some average population $\overline{y}$. Intuitively, because migration is symmetric and dominates both the growth and loss terms (when $\overline{y}_\alpha$ is small), the balance of migration – to and from – forces the mean of all subpopulations to be equal in steady state. Even subgroups with zero (or negative) μ, that if isolated would have gone extinct, are replenished by migration from the reproducing classes, as long as the migration strength is nonzero.

Including small variations, $(\overline{y}_\alpha - \overline{y})/\overline{y} \ll 1$, among the different classes, we linearize Eq. (3.2) around $\overline{y}$ to find the average population (full derivation in Appendix A).

$$\begin{aligned} \overline{y} &= \left(\frac{\sum_\alpha p_\alpha \mu_\alpha}{p_{\alpha_0} \gamma_{\alpha_0} \sum_\beta D_{\alpha_0 \beta} p_\beta}\right)^{1/q_{\alpha_0}} , \\ \alpha_0 &\equiv \arg\min_\alpha \, q_\alpha . \end{aligned} \tag{3.4}$$

Interestingly, this result implies that as the mean production rate vanishes, the mean population goes extinct as $\overline{y} \propto \overline{\mu}^\beta$ with exponent $\beta = 1/q_{\alpha_0}$. Thus, the fate of the entire population (as quantified by the critical exponent) is linked neither to the subpopulation with the largest or smallest fitness nor the largest subpopulation (with the highest p_α), but to the subpopulation with the largest noise-to-migration ratio (α_0). The larger this ratio, the higher the critical exponent and the faster the average population decays.

To gain insight into this delicate dependence on an exotic subpopulation, we consider Eq. (2.11) in the extinction limit. The growth term on the left admits an effective growth rate $\left(\sum_\alpha p_\alpha \mu_\alpha\right) \overline{y}$, which behaves similarly in the limit $\overline{y} \to 0$ for all subpopulations. However, unlike the means, the second moments behave differently. We use Eq. (4.4) to find

$$\langle y_\alpha^2 \rangle \propto \begin{cases} \overline{y}^2 & \text{for } \omega_\alpha > 1 , \\ \overline{y}^{1+\omega_\alpha} & \text{for } \omega_\alpha < 1 . \end{cases} \tag{3.5}$$

The difference in the scaling law of the second moments suggests that for a small population size, the population loss from class α_0 with the smallest ω_α dominates the loss from other subpopulations, hence the importance of class α_0 in Eq. (3.4).

4. Generalized growth law

We next consider the evolution of the population size with time. Absent an explicit solution to the time-dependent Fokker-Planck equation, we appeal to a 'seasonal growth model' in which a population alternates between two distinct behaviors, separating an on-site reproduction phase from a stochastic exploration phase. As shown below, this model motivates the usage of a quasi-steady state and therefore Eq. (2.11).

Let us assume that during the stochastic exploration phase, there is no reproduction and the population changes only through the linear terms: migration and seascape noise. After a sufficiently long time, the population reaches a steady distribution described by Eq. (2.8) for $C_{\mu_\alpha} = C_{a_\alpha} = 0$, given by

$$\hat{\rho}_\alpha(y_\alpha) = y_\alpha^{-2-C_{D_\alpha}} e^{-C_{D_\alpha}\frac{(y_0)_\alpha}{y_\alpha}} \ , \tag{4.1}$$

an inverse, scaled Cauchy distribution with mean $(y_0)_\alpha$. As before, self-consistency requires $\overline{y}_\alpha = (y_0)_\alpha$, consistent with the condition imposed by the balance of migration: $\overline{y}_\alpha = \overline{y}$ for all α and some $\overline{y}$ (All subpopulations have the same mean by the end of the exploration phase, since without growth, the net flux between any two classes, $D_{\alpha\beta}N_\alpha N_\beta/\mathcal{N}\left|\overline{y}_\alpha - \overline{y}_\beta\right|$, has to vanish in steady state).

Note the absence of an upper cutoff in Eq. (4.1) due to neglect of the saturating nonlinearities. In actuality, there will be an upper cutoff Λ_α set by the duration of the exploration phase. We also impose a lower cutoff Υ_α to implement the self-consistency condition, approximating to a pure power-law distribution

$$\hat{\rho}(y_\alpha) \propto \begin{cases} y_\alpha^{-2-C_{D_\alpha}} & \text{for } \Upsilon_\alpha < y_\alpha < \Lambda_\alpha \ , \\ 0 & \text{otherwise} \ . \end{cases} \tag{4.2}$$

As long as $\Lambda_\alpha \gg \Upsilon_\alpha$, the mean of the distribution is $\langle y\rangle = (1 + C_{D_\alpha})\Upsilon_\alpha/C_{D_\alpha}$, so we set

$$\Upsilon_\alpha = \frac{C_{D_\alpha}}{1 + C_{D_\alpha}} \langle y_\alpha\rangle \ . \tag{4.3}$$

We then integrate over Eq. (4.2) to find the m-th moment, which has two distinct behaviors depending on the value of C_{D_α}:

$$\langle y_\alpha^m\rangle \propto \begin{cases} \langle y_\alpha\rangle^{1+C_{D_\alpha}} & \text{for } 0 < C_{D_\alpha} < m-1 \ , \\ \langle y_\alpha\rangle^m & \text{for } C_{D_\alpha} > m-1 \ . \end{cases} \tag{4.4}$$

For small C_{D_α}, with seascape noise dominating migration, nonanalytic behavior arises, initially for the higher moments. The leading nonlinearity, however, remains as $\langle y\rangle^2$ until $C_{D_\alpha} < 1$, where it is replaced by $\langle y\rangle^{1+C_{D_\alpha}}$. Importantly, in this regime, all higher moments (and hence any analytic function) have average dependence as $\langle y\rangle^{1+C_{D_\alpha}}$.

The evolution of $\overline{y}_\alpha(t)$ during the reproduction phase is governed by the local growth and saturation terms $\mu_\alpha y_\alpha + S(y)$. This has to be averaged over the stationary distribution from the prior exploration phase, and in particular the moments $\langle y_\alpha^m\rangle$ from Eq. (4.4). In a short growth time, we find

$$\Delta\langle y_\alpha(t)\rangle \simeq (\mu_\alpha \langle y_\alpha(t)\rangle - a_\alpha \langle y_\alpha^2(t)\rangle + \cdots)\,\Delta t \ , \tag{4.5}$$

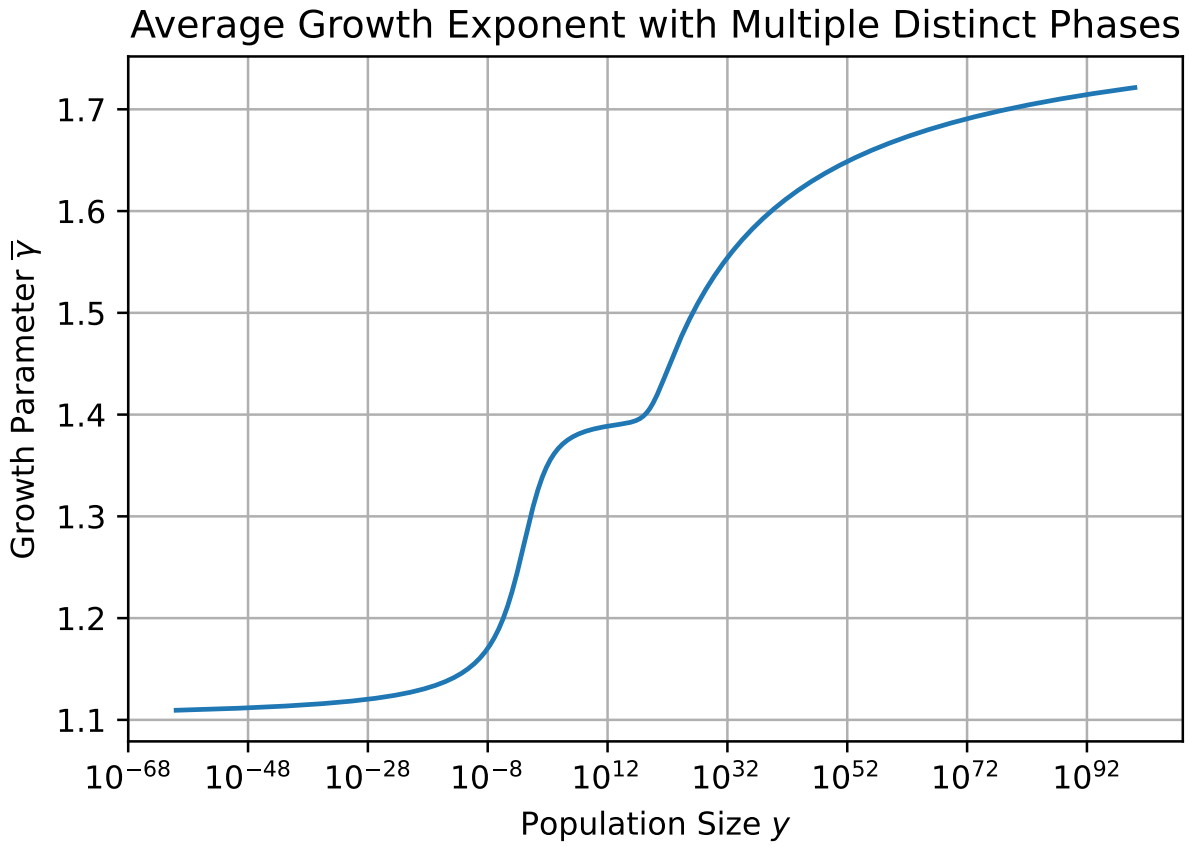

Figure 1. The average exponent $\overline{\gamma}$ from the Richards growth model (defined in Eq. (4.9)) for a system with three subpopulations – 10^{-6}% with $\gamma_1 = 1.8$, 20% with $\gamma_2 = 1.4$, and 80% with $\gamma_3 = 1.1$. Three distinct regimes are visible. For small population size, the largest subpopulation contributes the most, so $\overline{\gamma} \approx 1.1$. For a larger population size, the more exotic subpopulations have more effect, and $\overline{\gamma}$ increases to 1.4 and 1.8.

to first order in Δt, or equivalently,

$$\begin{aligned} \frac{\Delta\langle y_\alpha(t)\rangle}{\Delta t} &= \mu_\alpha \langle y\rangle \left(1 + (-A_\alpha + \cdots)\langle y\rangle^{C_{D_\alpha}}\right) \ , \\ A_\alpha &\equiv \frac{C_{D_\alpha} a_\alpha \Lambda_\alpha}{1 - C_{D_\alpha}} \left[\frac{C_{D_\alpha}}{(1 + C_{D_\alpha})\Lambda_\alpha}\right]^{C_{D_\alpha}} \ , \end{aligned} \tag{4.6}$$

where we already substituted in $\langle y_\alpha\rangle = \langle y\rangle$; the amplitudes arising from the higher order terms of $S(y)$ can be calculated in a similar manner. This leads to a change in the overall population by the end of a growth phase, according to

$$\overline{y}(t + \Delta t) = \sum_\alpha p_\alpha \overline{y}_\alpha(t + \Delta t) \ . \tag{4.7}$$

The growth law for the entire population then takes the form

$$\frac{\partial \overline{y}(t)}{\partial t} = \sum_{\alpha} p_\alpha \mu_\alpha \, \overline{y}(t) - \sum_{\alpha} p_\alpha A_\alpha \, \overline{y}^{C_{D_\alpha}+1}(t) \ , \tag{4.8}$$

returning the form of Eq. (2.11).

While for a single class, the above result amounts to a justification of the Richards growth law, for multiple classes the growth law is no longer simple and can include the sum of multiple fractional growth terms. As $\overline{y}$ increases, smaller subpopulations (smaller p_α) with larger exponent start to make appearance. As a specific example, Figure 1 depicts the variation of an effective Richards exponent for a population with three classes, defined through

$$\overline{A} \ \overline{y}^{\overline{\gamma}} = \sum_{\alpha} p_\alpha \left[A_\alpha y^{\gamma_\alpha} \right] \ , \ \text{with} \ \overline{A} \equiv \sum_{\alpha} p_\alpha \left[A_\alpha \right] \ . \tag{4.9}$$

5. Conclusions

Given the diverse contexts for dynamics of evolving populations, it is important to explore the influence of variability at different times and locations. This paper expands on previous works [22, 23] in which variations in reproduction rate at different locations and times were considered in the form of independent random noise. However, apart from this (seascape) noise, the different locations were treated identically in their growth, saturation, and migration rates. This assumption made the problem analytically tractable by a self-consistent (mean-field) approach. In this paper, we introduce a specific form of inhomogeneity, by considering ℓ subpopulations with distinct average growth and saturation rates, different scales of seascape noise as well as pair-wise migration rates.

The choice of model allows a generalization of the mean-field approach, with ℓ self-consistent equations describing the subpopulation means $\{\overline{y}_\alpha\}$ and corresponding distributions $\{\hat{\rho}_\alpha(y_\alpha)\}$. To make sense of the results, let us note that for an isolated population, seascape noise leads to a broad log-normal distribution $\hat{\rho}(y)$. Migration between sites and saturation effects tame the log-normal distribution to a power-law form (in the long-time limit as supported by steady-states of the Fokker–Plank equation). The easiest limit to justify analytically is in a quasi-steady state and when migration and seascape noise are the dominant effects. The symmetric migration assumed in this work then makes all subpopulations have the same average $\overline{y}_\alpha = \overline{y}$ (to zeroth order), while their respective distributions can be described by different power-laws. We can then follow the behavior of the single parameter $\overline{y}$ in two cases of extinction and growth:

In the steady-state (long time) limit, extinction occurs when the mean reproduction rate vanishes. If the average reproduction rate $\overline{\mu} = \sum_\alpha p_\alpha \mu_\alpha$ is nonnegative, the growing subpopulations act as sources to the decaying subpopulations through migration. As $\overline{\mu} \to 0$, the common average population vanishes as $\overline{y} \propto \overline{\mu}^\beta$. For noiseless logistic growth $\beta = 1$, while seascape and migration modify the exponent to a fractional $\beta < 1$. Interestingly, the value of the exponent β does not depend on the population with the largest fitness, or on the subpopulation with the largest number of members. Rather, it is dominated by the subpopulation with the largest noise-to-migration ratio. Effectively, this subpopulation acts as a sink that rapidly diminishes the overall population.

Another interesting case is that of the growth of the average population $\overline{y}(t)$ to its final value. For a single population, it was shown in Reference [23] that for a sufficient slow growth, the evolution

of $\overline{y}(t)$ is described by the Richards law with a fractional exponent. In the inhomogenous case, the overall growth is no longer described by a single fractional exponent, but rather by effective exponents appearing at different scales, moving to larger values as the population size increases.

It is tempting to infer connections between our results and real world situations such as pandemic modeling. Our results certainly indicate that noise and inhomogeneity can profoundly affect population dynamics and lead to novel phenomena. However, various simplifying assumptions of the model (such as symmetric migration, limiting inhomogeneity to a finite number of subgroups, ignoring demographic noise, etc.) are also likely to constrain its applicability. Further work to go beyond these limitations is certainly called for.

Acknowledgements

T.T. thanks Average Phan, Vincent Bian, and Albert Qin for their feedback. M.K. is supported in part by NSF grant No. DMR-1708280.

References

[1] P. Gerlee, "The model muddle: in search of tumor growth laws," *Cancer research* **73** (2013) 2407.

[2] D. Fekedulegn, M. P. Mac Siúrtáin, and J. J. Colbert, "Parameter Estimation of Nonlinear Models in Forestry," *Silva Fennica* **33** (1999) 327.

[3] K. Wu, D. Darcet, Q. Wang, and D. Sornette, "Generalized logistic growth modeling of the COVID-19 outbreak: comparing the dynamics in the 29 provinces in China and in the rest of the world," *Nonlinear dynamics* **101** (2020) 1561.

[4] J. Kemp and L. Bettencourt, "*Statistical Dynamics of Wealth Inequality in Stochastic Models of Growth*," *Physica A: Statistical Mechanics and its Applications* **607** (2022) 128180.

[5] Y. Hao, T. Xu, H. Hu, P. Wang, and Y. Bai, "Prediction and analysis of corona virus disease 2019," *PloS one* **15** (2020) e0239960.

[6] M. E. Turner Jr, E. L. Bradley Jr, K. A. Kirk, and K. M. Pruitt, "A theory of growth," *Mathematical Biosciences* **29** (1976) 367.

[7] T. Royama, "Analytical population dynamics," Springer Science & Business Media, U.K, (1992).

[8] R. Haberman, Mathematical models: mechanical vibrations, population dynamics, and traffic flow. Society for Industrial and Applied Mathematics, U.S.A., (1998).

[9] P. Turchin, "Complex population dynamics," Princeton University Press, U.S.A, (2013).

[10] M. A. Nowak, Evolutionary dynamics: exploring the equations of life," Belknap Press, U.S.A., (2006).

[11] A. S. Martinez, R. S. González, and C. A. S. Terçariol, "Continuous growth models in terms of generalized logarithm and exponential functions," *Physica A: Statistical Mechanics and its Applications* **387** (2008) 5679.

[12] A. Tsoularis and J. Wallace, "*Analysis of logistic growth models*," *Mathematical Biosciences* **179** (2002) 21–55.

[13] R. Durrett and S. Levin, "The importance of being discrete (and spatial)," *Theoretical Population Biology* **46** (1994) 363.

[14] A. Traulsen, J. C. Claussen, and C. Hauert, "Stochastic differential equations for evolutionary dynamics with demographic noise and mutations," *Physical Review E* **85** (2012) 041901.

[15] H. Weissmann, N. M. Shnerb, and D. A. Kessler, "Simulation of spatial systems with demographic noise," *Physical Review E* **98** (2018) 022131.

[16] M. Parker, A. Kamenev, and B. Meerson, "Noise-induced stabilization in population dynamics," *Physical Review Letters* **107** (2011) 180603.

[17] G. W. Constable, T. Rogers, A. J. McKane, and C. E. Tarnita, "Demographic noise can reverse the direction of deterministic selection," *Proceedings of the National Academy of Sciences* **113** (2016) E4745.

[18] T. Butler and N. Goldenfeld, "Robust ecological pattern formation induced by demographic noise," *Physical Review E* **80** (2009) 030902.

[19] T. Agranov and G. Bunin, "Extinctions of coupled populations, and rare event dynamics under non-Gaussian noise," *Physical Review E* **104** (2021) 024106.

[20] R. Lande, "Risks of population extinction from demographic and environmental stochasticity and random catastrophes," *The American Naturalist* **142** (1993) 911–927.

[21] F. Ginelli, V. Ahlers, R. Livi, D. Mukamel, A. Pikovsky, A. Politi, and A. Torcini, "From multiplicative noise to directed percolation in wetting transitions," *Physical Review E* **68** (2003) 065102.

[22] B. Ottino-Löffler and M. Kardar, "Population extinction on a random fitness seascape," *Physical Review E* **102** (2020) 052106.

[23] D. W. Swartz, B. Ottino-Löffler, and M. Kardar, "Seascape origin of Richards growth," *Physical Review E* **105** (2022) 014417.

[24] F. Richards, "A flexible growth function for empirical use," *Journal of experimental Botany* **10** (1959) 290.

[25] A. Werker and K. Jaggard, "Modelling asymmetrical growth curves that rise and then fall: Applications to foliage dynamics of sugar beet (Beta vulgaris L.)," *Annals of Botany* **79** (1997) 657–665.

[26] A. Gregorczyk, "Richards plant growth model," *Journal of Agronomy and Crop Science* **181** (1998) 243.

[27] M. Materassi, "Some fractal thoughts about the COVID-19 infection outbreak," *Chaos, Solitons & Fractals: X* **4** (2019) 100032.

[28] G. Chowell, D. Hincapie-Palacio, J. Ospina, B. Pell, A. Tariq et al., "Using phenomenological models to characterize transmissibility and forecast patterns and final burden of Zika epidemics," *PLoS Currents* **8** (2016).

[29] K. Roosa, Y. Lee, R. Luo, A. Kirpich, R. Rothenberg et al., "Real-time forecasts of the COVID-19 epidemic in China from February 5th to February 24th, 2020," *Infectious Disease Modelling* **5** (2020) 256.

[30] R. K. Singh, M. Rani, A. S. Bhagavathula, R. Sah, A. J. Rodriguez-Morales et al., "Prediction of the COVID-19 pandemic for the top 15 affected countries: Advanced autoregressive integrated moving average (ARIMA) model," *JMIR Public Health and Surveillance* **6** (2020) e19115.

[31] M. Zwietering, I. Jongenburger, F. Rombouts, and K. Van't Riet, "Modeling of the bacterial growth curve," *Applied and Environmental Microbiology* **56** (1990) 1875–1881.

[32] V. Mahajan, E. Muller, and F. M. Bass, "New product diffusion models in marketing: A review and directions for research," *Journal of Marketing* **54** (1990) 1.

[33] M. Haddon, "Modelling and quantitative methods in fisheries," Chapman and Hall/CRC, U.S.A., (2011).

[34] A. D. MacCall, "Dynamic geography of marine fish populations," University of Washington Press, U.S.A., (1989).

[35] D. Pauly, "On the interrelationships between natural mortality, growth parameters, and mean environmental temperature in 175 fish stocks," *ICES journal of Marine Science* **39** (1980) 175.

[36] J. K. Vanclay, "Modelling forest growth and yield: applications to mixed tropical forests," Cab International, U.K., (1994).

[37] H. Pretzsch, "Forest dynamics, growth, and yield," Springer-Verlag, Germany, (2009).

[38] J. Liu and P. S. Ashton, "Individual-based simulation models for forest succession and management," *Forest ecology and management* **73** (1995) 157.

[39] O. Garcia, "A stochastic differential equation model for the height growth of forest stands," *Biometrics* **39** (1983) 1059.

[40] R. Mead, R. N. Curnow, and A. M. Hasted, "Statistical methods in agriculture and experimental biology," Chapman and Hall/CRC, Boca Raton, (2017).

[41] S. Paterson and B. A. Bryan, "Food-carbon trade-offs between agriculture and reforestation land uses under alternate market-based policies," *Ecology and Society* **17** (2012).

[42] C. Van den Broeck, J. Parrondo, J. Armero, and A. Hernández-Machado, "Mean field model for spatially extended systems in the presence of multiplicative noise," *Physical Review E* **49** (1994) 2639.

[43] C. Van den Broeck, J. Parrondo, and R. Toral, "Noise-induced nonequilibrium phase transition," *Physical Review Letters* **73** (1994) 3395.

[44] J. Desponds, T. Mora, and A. M. Walczak, "Fluctuating fitness shapes the clone-size distribution of immune repertoires," *Proceedings of the National Academy of Sciences* **113** (2016) 274.

[45] P. Lombardo, A. Gambassi, and L. Dall'Asta, "Nonmonotonic effects of migration in subdivided populations," *Physical Review Letters* **112** (2014) 148101.

[46] S. N. Gomes and G. A. Pavliotis, "Mean field limits for interacting diffusions in a two-scale potential," *Journal of Nonlinear Science* **28** (2018) 905.

[47] E. F. Heffern, H. Huelskamp, S. Bahar, and R. F. Inglis, "Phase transitions in biology: from bird flocks to population dynamics," *Proceedings of the Royal Society B* **288** (2021) 20211111.

[48] D. C. Markham, M. J. Simpson, P. K. Maini, E. A. Gaffney, and R. E. Baker, "Incorporating spatial correlations into multispecies mean-field models," *Physical Review E* **88** (2013) 052713.

[49] S. Gibaud and J. W. Weibull, "Accumulation of individual fitness or wealth as a population game," arXiv:1707.00996 (2017).

[50] T. V. Phan, R. Morris, M. E. Black, T. K. Do, K.-C. Lin et al., "Bacterial route finding and collective escape in mazes and fractals," *Physical Review X* **10** (2020) 031017.

Appendix

A. Deriving extinction mean

In this appendix, we provide an analytic solution to Eq. (3.2), to first order approximation.

We linearize this system of equations around $\overline{y}$, to solve for both the average population $\overline{y}$ as well as the subleading corrections, by setting

$$\overline{y}_\alpha = \overline{y}\,(1+f_\alpha)\,. \tag{A.1}$$

Here, $\overline{y}$ is the zeroth order approximation such that all the first order corrections $f_\alpha \propto \Delta\mu$, the variations of μ_α, as $\mu \to 0$ satisfy $f_\alpha \ll 1$ (so there is freedom to choose a constraint $\mathcal{F}\{f_\alpha\} = 0$). Combining Eq. (3.2) and Eq. (A.1) gives

$$f_\alpha - \frac{\sum_\beta C_{D_{\alpha\beta}} p_\beta f_\beta}{C_{D_\alpha}} = \frac{C_{\mu_\alpha}}{C_{D_\alpha}} - \gamma_\alpha (y_0)_\alpha^{q_\alpha}\ , \tag{A.2}$$

a set of coupled linear equations for f_β.

The average population $\overline{y}$ can be solved separately from the corrections f_α. Multiplying both sides of Eq. (A.2) by $p_\alpha C_{D_\alpha}\sigma_\alpha^2/2$ and summing over all α gives

$$\begin{aligned}&\sum_{\alpha\beta} D_{\alpha\beta} p_\alpha p_\beta (f_\alpha - f_\beta)\\ &= \sum_\alpha p_\alpha \mu_\alpha - \sum_{\alpha\beta} D_{\alpha\beta} p_\alpha p_\beta \gamma_\alpha (y_0)_\alpha^{q_\alpha}\ .\end{aligned} \tag{A.3}$$

The left-hand side of the above equation vanishes because $D_{\alpha\beta}$ is symmetric. For the right-hand side, to first order, we replace $(y_0)_\alpha$ with $\overline{y}$. Moreover, as the limit of $\overline{y} \to 0$, only the term with the smallest exponent, q_{α_0} corresponding to class α_0, contributes to the sum over α. Omitting the other terms gives:

$$\begin{aligned}\overline{y} &= \left(\frac{\sum_\alpha p_\alpha \mu_\alpha}{p_{\alpha_0}\gamma_{\alpha_0}\sum_\beta D_{\alpha_0\beta} p_\beta}\right)^{1/q_{\alpha_0}}\ ,\\ \alpha_0 &\equiv \arg\min_\alpha\ q_\alpha\ .\end{aligned} \tag{A.4}$$

We find the corrections f_α by directly solving the set of linear equations in Eq. (A.2). We use the constraint to set $f_{\alpha_0} = 0$ and obtain the following solution:

$$\begin{aligned}\overline{y} &= \left(\frac{\sum_{\beta\neq\alpha_0} A_{\alpha_0\beta} f_\beta + C_{\mu_{\alpha_0}}}{\gamma_{\alpha_0} C_{D_{\alpha_0}}}\right)^{1/q_{\alpha_0}}\ ,\\ f_\beta &= \begin{cases} 0 & \text{if } \beta = \alpha_0 \\ (A^{-1}B)_\beta & \text{otherwise}\end{cases}\ ,\end{aligned} \tag{A.5}$$

with the following short-hand notations:

$$\begin{aligned}\alpha_0 &\equiv \arg\min\ q_\alpha\ ,\\ A_{\alpha\beta} &\equiv \delta_{\alpha\beta} - C_{D_{\alpha\beta}} p_\beta / C_{D_\alpha}\ ,\ \alpha \neq \alpha_0\ ,\\ B_\alpha &\equiv C_{\mu_\alpha}/C_{D_\alpha}\ ,\ \alpha \neq \alpha_0\ .\end{aligned} \tag{A.6}$$

The two obtained expressions for $\overline{y}$ are equivalent, and the last step is to verify if all the $f_\alpha \ll 1$.

B. A different scheme

There is an alternative interpretation of the logistic equation, in which the parameters a_α are functionally related to μ_α. In the standard scheme, a_α is entirely independent of μ_α, and by varying μ_α, we also vary the capacity of the population. In the alternative scheme, population capacity K is kept fixed, and the logistic growth equation takes the form

$$\frac{\mathrm{d}y}{\mathrm{d}t} = \mu y \left(1 - \frac{y}{K}\right) \ , \tag{B.1}$$

which sets $a = \mu/K$.

First, we discuss the difference in extinction behaviors of the two alternative schemes, focusing on the one class case for simplification. Without seascape noise, Eq. (B.1) implies that the steady state population makes a discontinuous jump:

$$y = \begin{cases} K & \text{if } \mu > 0 \ , \\ 0 & \text{if } \mu = 0 \ . \end{cases} \tag{B.2}$$

However, in the absence of demographic noise, the existence of large seascape noise, where $\sigma^2 > 2(D-\mu)$, makes the transition continuous:

$$\begin{aligned} \overline{y} &= K \cdot \frac{\sigma^2}{4D} \left[\frac{-\Gamma(1+\omega)}{D\,\omega\,\Gamma(-\omega)}\right]^{1/\omega} \cdot \mu^{1/\omega - 1} \ , \\ \omega &= \frac{2(D-\mu)}{\sigma^2} \ . \end{aligned} \tag{B.3}$$

obtained by letting $a_\alpha \propto \mu_\alpha$ in Eq. (3.4). Figure 2 indicates that the closer σ^2 is to $2D$, the sharper the transition.

The choice of a scheme also has important impact on the factional growth obtained in this paper. For the second scheme in Eq. (B.1), a stochastic, uncorrelated noise $\eta(t)$ added to μ not only generates the seascape term proportional to y, but also an additional noise term proportional to y^2. This extra noise term changes the power law behavior for the large tail of the population distribution, and the investigation of such a noise term will be deferred to the future.

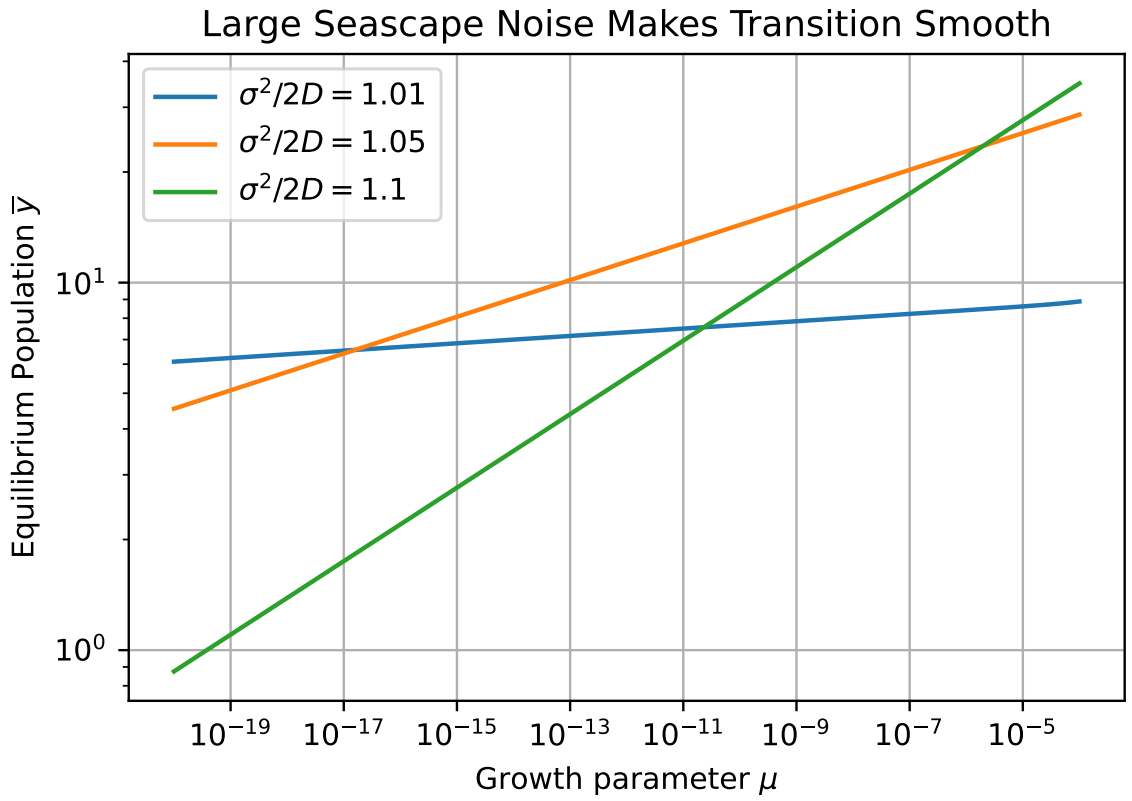

Figure 2. Equilibrium population $\overline{y}$ versus growth parameter in the fixed-capacity model (visualization of equation Eq. (B.3)). The curves for all three values of $\sigma^2/2D$ are negative, indicating a slow extinction transition from the capacity K to zero. The smaller $\sigma^2/2D$ is, the less negative the slope is and the harder it is to observe the extinction phase.